Substrate Binding Determinants of *Trypanosoma brucei* γ-Glutamylcysteine Synthetase†

Jared J. Abbott, Jennifer L. Ford, and Margaret A. Phillips*

Department of Pharmacology, The University of Texas Southwestern Medical Center at Dallas, 5323 Harry Hines Boulevard, Dallas, Texas 75390-9041

Received November 2, 2001; Revised Manuscript Received January 2, 2002

ABSTRACT: γ-Glutamylcysteine synthetase (γ-GCS) catalyzes the ATP-dependent ligation of L-Glu and L-Cys, which is the first step in de novo biosynthesis of the tripeptide glutathione. Recently it was demonstrated that γ-GCS is a structural homologue of glutamine synthetase (GS), providing the basis to build a model for the γ-GCS active site [Abbott et al. (2001) *J. Biol. Chem. 276*, 42099−42107]. Substrate binding determinants in the active site of γ-GCS have been identified and characterized in the enzyme from the parasitic protozoa *Trypanosoma brucei* using this model as a guide for site-directed mutagenesis. R366 and R491 were identified as key determinants of L-Glu binding. Mutation of R366 to Ala increases the K_d for L-Glu by 160-fold and eliminates the positive cooperativity observed for the binding of L-Glu and ATP to the wild-type enzyme, based on a rapid equilibrium random mechanism of substrate binding. Unlike the wild-type enzyme, the R366A mutant enzyme was able to form product using the substrate analogue γ-aminobutyric acid, suggesting that R366 interacts with the α-carboxylate of L-Glu. Mutation of R491 to Ala decreased k_{cat} for ATP hydrolysis by 70-fold; however, dipeptide product was only formed in 5% of these turnovers. These data suggest that R491 stabilizes the phosophorylated γ-carboxylate of L-Glu during nucleophilic attack by the L-Cys to form the dipeptide product. T323, R474, and R487 were predicted to be ATP binding determinants. Mutation of each of these residues to Ala increased the apparent K_m for ATP by 20−100-fold while having only modest effects on k_{cat} or the apparent K_m's for the other substrates. Finally, mutation of R179, a conserved residue that is present in γ-GCS, but not in GS, increased the apparent K_m for both L-Cys and L-Glu.

γ-Glutamylcysteine synthetase (γ-GCS)[1] catalyzes the ATP-dependent ligation of L-Cys to L-Glu (Scheme 1), which is the first committed step in the biosynthesis of the tripeptide thiol glutathione (GSH) (*1*). Unlike in mammalian cells, trypanosomes conjugate GSH to spermidine to form a novel cofactor, trypanothione. This cofactor is maintained in the reduced state by the action of trypanothione reductase, a homolgue of glutathione reductase (*2*). Trypanosomes rely heavily on cellular stores of trypanothione to prevent oxidative injury by peroxides (*3*), thereby making the biosynthetic pathway of trypanothione a potential target for drug development. Indeed, a specific inhibitor of γ-GCS, L-buthionine sulfoximine (L-BSO), can cure *Trypanosoma brucei* infections in mice (*4*). *T. brucei* γ-GCS has been cloned, expressed, and characterized (*5*). The kinetic mechanism of *T. brucei* γ-GCS has been modeled by a rapid equilibrium random ter-reactant system (*6*).

Scheme 1

$$\text{L-Glu} + \text{L-Cys} + \text{ATP} \xrightleftharpoons[Mg^{2+}]{\gamma\text{GCS}} \text{L-}\gamma\text{-glutamyl-cysteine} + \text{ADP} + P_i$$

Studies on mammalian γ-GCS suggest that the reaction mechanism proceeds through a γ-glutamyl phosphate intermediate, which is attacked by the α-amino group of L-Cys to form the dipeptide product (*1*). Furthermore, it was found that γ-GCS can catalyze partial reactions such as ATP hydrolysis or cyclization of L- or D-Glu (*7*). Supporting the idea of a phosphorylated intermediate, L-BSO is phosphorylated by γ-GCS to form a tight binding transition-state analogue (*8*, *9*). Analysis of substrate specificity in mammalian γ-GCS reveals that the L-Glu binding site requires a 5-carbon molecule, both carboxylate groups, and the α-amino group. D-Glu stimulates ATP hydrolysis activity in the rat γ-GCS enzyme but does not participate in dipeptide product formation, while the L-Glu analogue, γ-aminobutyrate (GABA), did not stimulate ATP hydrolysis in the rat γ-GCS holoenzyme at any detectable rate (*10*). The L-Cys binding site is considerably more promiscuous. L-α-Aminobutyrate (L-Aba), along with several other amino acids such as L-norvaline and DL-homocysteine, can serve as alternate acceptor amino acids (*7*).

† This work was supported by grants from the National Institutes of Health (R01 AI34432) and the Welch Foundation (I-1257) (to M.A.P.) and by National Institutes of Health Medical Scientist Training Program Grant T32-GM08014 (to J.J.A.). M.A.P. is a recipient of a Burroughs Wellcome Fund Scholar Award in Molecular Parasitology.

* To whom correspondence should be addressed. Tel: (214) 648-3637. Fax: (214) 648-9961. Email: Margaret.Phillips@UTSouthwestern.edu.

[1] Abbreviations: γ-GCS, γ-glutamylcysteine synthetase; GS, glutamine synthetase; GSH, glutathione; mutant enzymes are designated by single-letter amino acid codes and residue number, e.g., R366A is the Arg366 to Ala mutant *T. brucei* γ-GCS; L-BSO, L-buthionine sulfoximine; GABA, γ-aminobutyric acid; L-Aba, L-α-aminobutyrate; GABA-Aba, dipeptide of GABA and L-Aba; PCR, polymerase chain reaction; HPLC, high-pressure liquid chromatography; RT, retention time.

10.1021/bi0159128 CCC: $22.00
Published on Web 02/01/2002

The structural basis for substrate binding in the γ-GCS family has not been characterized. We recently demonstrated that γ-GCS is a structural homologue of the C-terminal domain of glutamine synthetase (GS) (*11*). The X-ray structures for GS bound to a number of substrates and inhibitors have been solved (*12*), providing the basis for generating a model of the γ-GCS active site. Two Mg^{2+} binding sites were identified by this analysis, and mutagenesis of the six metal binding residues demonstrated that the metals play key roles in catalysis and substrate binding in the γ-GCS family (*11*). The structural prediction also identified several residues with potential roles in binding of L-Glu and ATP. The X-ray structures of GS identify two Arg residues that interact with L-Glu: R321 binds the α-carboxylate of L-Glu, and R359 is involved in binding the γ-carboxylate of L-Glu (*13, 14*). ATP has several identified binding determinants in GS: the n2 metal chelates the γ-phosphate of ATP, R344 coordinates the β-phosphate of ADP, and H271 coordinates the α-phosphate of ADP (*13*). The multiple sequence alignment of GS and γ-GCS (Figure 1) reveals that these ATP and L-Glu substrate binding residues of GS are largely conserved in γ-GCS (*11*).

While GS and γ-GCS share many similarities in their reaction chemistry, the third substrate differs; thus, the GS structure provides less insight into the L-Cys binding site in γ-GCS than for the other substrates. GS, which is a dodecamer, binds ammonia as the third ligand utilizing a residue (Asp50) from the N-terminus of an adjacent subunit as part of the binding site (*15*). In contrast, gel filtration studies on *T. brucei* γ-GCS indicate that γ-GCS exists as a monomer (*5*), suggesting that γ-GCS must use a different mechanism to bind its third ligand.

In this paper, we identify and characterize the roles of amino acid residues that influence the kinetic properties of the three substrates in the reaction catalyzed by *T. brucei* γ-GCS. Seven conserved residues were mutated to Ala, and the kinetic behavior of the mutant enzymes was analyzed. These data make novel observations about binding determinants for all three substrates and two important inhibitors, GSH and L-BSO. R366 is a crucial residue for L-Glu binding, and it mediates cooperative interactions between L-Glu, ATP, and L-Aba. R491 plays a role in catalyzing peptide bond formation. The GS-based model of the γ-GCS structure predicts that T323, R474, and R487 are ATP binding determinants. In support of this hypothesis, mutation of each of these residues to Ala in γ-GCS significantly increases the K_m^{app} for ATP. Finally our studies identify R179 as a possible binding determinant for either L-Aba or L-Glu. These data provide key insights regarding the residues that control substrate binding and catalysis in the active site of *T. brucei* γ-GCS.

EXPERIMENTAL PROCEDURES

Materials. All reagents for the enzyme assay were purchased from Sigma; Ni^{2+}-agarose and pREP4 were purchased from Qiagen. The GABA-Aba dipeptide (peptide bond between the γ-carboxylate of GABA and the α-amino group of L-Aba) was custom-synthesized by American Peptide Co. (Sunnyvale, CA).

Mutagenesis. PCR-based mutagenesis of the *T. brucei* γ-GCS expression vector was performed using the QuickChange site-directed mutagenesis kit from Stratagene. The primers (Genosys) consist of the 5′-3′ primer (below) and the exact complement, with the replaced codon underlined: R179A, 5′-GCGTGTATCAATGATTCTCATCCTGCTTTGAAGGCTCTCACG-3′; T323A, 5′-GCTGCAACTGCCTTCAGCTTGCCATGCAGCTTCCTAATGAAGC-3′; R366A, 5′-GCGAGTCGGACGTTGCCTGGTGACGATCACCG-3′; R474A, 5′-GCACAAATTGGCAAACTGTTGCTTTGAAACTTCCCGTGCTTGACAGC-3′; R487A, 5′-GCACGCTTGGGTGGGCTGTGGAGTTTCGTGAATGG-3′; R491A, 5′-GGGTGGCGTGTGGAGTTTGCTGTAATGGACGTGATGCC-3′. The full coding region was sequenced for each mutant plasmid to confirm the constructs.

Expression and Purification. *T. brucei* γ-GCS was expressed as a C-terminal His_8-tag fusion in a T7 bacterial (BL21/DE3 cells cotransformed with pREP4) expression vector. Protein was purified over a Ni^{2+}-agarose column, as described (*6*). The wild-type, R366A, and T323A enzymes were further purified by gel filtration as described (*6*). Protein solutions were stored in 50 mM Tris, pH 8.0, 100 mM NaCl, 5 mM $MgCl_2$ at 4 °C. Protein concentration was determined by absorbance at 280 nm with a previously determined extinction coefficient (*6*).

Enzyme Assays. γ-GCS activity was measured at 37 °C with a spectrophotometric assay that couples ADP production to NADH oxidation (*5*). Substrate K_m^{app} and metal K_d^{app} data were collected and analyzed as described previously (*11*). Divalent metal in the form of $MgCl_2$ or $MnCl_2$ was added to the reaction over a range of free concentrations. The concentration of free metal was determined at a given total metal concentration, ATP concentration, and phosphoenolpyruvate concentration, under the conditions of the assay with the program 'Bound and Determined' (*16*). Unless otherwise stated, the following substrate and metal concentrations were used: 5 mM ATP, 100 mM L-Aba, 10 mM L-Glu, and 20 mM total $MgCl_2$. L-Aba was substituted for L-Cys in all kinetic assays. Enzyme concentration ranges were as follows: wild-type, 0.1−0.4 μM; R179A, R487A, and R474A, 0.4−3.0 μM; T323A, 0.8−2.0 μM with Mg^{2+} and 0.1−0.4 μM with Mn^{2+}; R366A and R491A, 3.0−12 μM.

For the GSH inhibition studies, GSH was added to the γ-GCS reaction at different concentrations, and L-Glu was varied over its dynamic concentration range while ATP and L-Aba were kept at constant, saturating levels. These data were fitted to the modified Michaelis−Menten equation for competitive inhibitors. L-BSO (1−5 μM for wild-type or 41 mM for R366A γ-GCS) was preincubated with enzyme and 5 mM ATP for 1−30 min. This mixture was added to the substrates to assay residual activity. The wild-type data were analyzed as described for a time-dependent inhibitor (*17*).

Analysis of Kinetic Mechanism. Data for wild-type γ-GCS were collected as described previously (*6*). R366A, R179A, R474A, and R487A mutant enzymes were tested over a range of substrate concentrations in which one substrate was held at a saturating level while the other two substrates are varied over their dynamic ranges. This process was repeated in all combinations until a matrix of data was collected. The data for R366A, R487A, and wild-type γ-GCS were fitted to eq 1, which describes a random, rapid-equilibrium ter-reactant system.

$$\nu/V_{\max} = \{[\mathrm{Glu}][\mathrm{Aba}][\mathrm{ATP}]/\alpha\beta\gamma K_{\mathrm{Glu}}K_{\mathrm{Aba}}K_{\mathrm{ATP}}\}/\{1 + [\mathrm{Glu}]/K_{\mathrm{Glu}} + [\mathrm{Aba}]/K_{\mathrm{Aba}} + [\mathrm{ATP}]/K_{\mathrm{ATP}} + [\mathrm{Glu}][\mathrm{Aba}]/\gamma K_{\mathrm{Glu}}K_{\mathrm{Aba}} + [\mathrm{Glu}][\mathrm{ATP}]/\beta K_{\mathrm{Glu}}K_{\mathrm{ATP}} + [\mathrm{Aba}][\mathrm{ATP}]/\alpha K_{\mathrm{ATP}}K_{\mathrm{Aba}} + [\mathrm{Glu}][\mathrm{Aba}][\mathrm{ATP}]/\alpha\beta\gamma K_{\mathrm{Glu}}K_{\mathrm{Aba}}K_{\mathrm{ATP}}\} \quad (1)$$

Chromatographic (HPLC) Analysis of γ-GCS Reaction Products. Wild-type, R366A, or R491A γ-GCS were incubated with L-Glu (10 mM for wild-type, 200 mM for R366A, and 20 mM for R491A) or GABA (100 mM for wild-type and 50 mM for R366A), L-Aba (20 mM for wild-type and R366A or 100 mM for R491A), and ATP (5 mM for wild-type and R366A or 3 mM for R491A) in buffer (40 mM MOPS, pH 8.0, 20 mM NaCl, and 5 mM $MgCl_2$) at 37 °C for a range of times. Enzyme concentrations were as follows: wild-type, 2−5 μM with L-Glu or 5−60 μM with GABA; R366A, 20−50 μM; and R491A, 15−35 μM. The reactions were stopped with the addition of TCA (final concentration of 7%). L-Asp (final concentration of 7.7 mM) was used as an internal standard. Aliquots of the samples (0.025 mL) were derivatized using the AccQ_TAG kit (Waters, Milford, MA) in buffer (170 mM MOPS, pH 8.0, 1.4 mM EDTA) plus reagent (0.031 mL of the AccQ_TAG kit reagent in a total volume of 0.125 mL) at 55 °C for 10 min. Sample (7 μL) was injected onto an AccQ_TAG column using published buffers and gradient (*18*). A Beckman System Gold HPLC was used, and peaks were monitored at 248 nm. The column was calibrated using standard samples of the following compounds, derivatized as above: L-Asp (RT = 17.1 min), L-Glu (RT = 19.7 min), L-Aba (RT = 28.6 min), GABA (RT = 28.1 min), γ-glutamylaminobutyrate (RT = 25.1 min), and GABA-Aba (RT = 29.1 min). The concentration of dipeptide product in the analyzed samples was determined from a standard curve generated from known concentrations of the compounds with respect to the internal standard. Rates of product formation were calculated from reaction mixtures in which the rate was linear with enzyme concentration.

Analytical Ultracentrifugation of Wild-Type γ-GCS. Sedimentation equilibrium data were collected in a Beckman XLI analytical ultracentrifuge. γ-GCS samples were analyzed in 50 mM Tris, pH 8, 100 mM NaCl, with no added metal, 5 mM total $MgCl_2$, or 25 μM total $MnCl_2$ at 20 °C. These metal concentrations were judged to be saturating conditions according to kinetic analysis. Three concentrations of γ-GCS (initial absorbance 0.15, 0.2, and 0.3) were loaded into a six sector equilibrium centerpiece and equilibrated (24 h) at three rotor speeds (8000, 10 000, and 12 000 rpm). Absorption data were collected through quartz window assemblies at 280 nm, using a radial step size of 0.001 cm and recorded as the average of 15 measurements at each radial position once samples were judged had reached equilibrium. The nine data sets for each enzyme were analyzed with the Beckman XL-A.XL-I Data Analysis Software Version 4.0 and globally fit using a monomer molecular weight of 80 000 and a molar extinction coefficient of 44 599 cm^{-1} M^{-1} to several models including monomer, dimer, trimer, tetramer, and monomer−dimer equilibrium. The baseline values were allowed to float, and v-bar (0.731 mL·g^{-1}) and ρ (1.00 g·mL^{-1}) were fixed during the fit to values determined using the program SEDNTERP (*19*). Goodness of fit was determined by examination of the residuals and minimization of the variance. The data were best fit to a monomer−dimer equilibrium in all cases.

RESULTS

Analysis of L-Glu Binding Determinants in T. brucei γ-GCS. The sequence alignments of GS and γ-GCS (Figure 1) in conjunction with the X-ray structures of GS bound to ligand (*13*, *20*) were used to identify the potential substrate binding residues in γ-GCS. The two Arg residues (GS R321 and GS R359) which interact with L-Glu in the GS structure are conserved in an amino acid sequence alignment of γ-GCS's and GS's (Figure 1). The analogous residues in *T. brucei* γ-GCS, R366, and R491, respectively, were mutated to Ala, expressed, and purified as described under Experimental Procedures. Kinetic analysis of the mutant enzymes, by the coupled spectrophotometric assay that follows ATP hydrolysis, demonstrates that both residues play important roles. For R366A γ-GCS, the largest effects were observed on the apparent K_m's (K_m^{app}) for L-Glu and ATP, which were increased by 540- and 40-fold, respectively, while the k_{cat} was reduced 12-fold and the K_m^{app} for L-Aba was unchanged (Table 1). For R491A γ-GCS, k_{cat} is 70-fold lower than for wild-type γ-GCS, while the apparent K_m for L-Glu increases

```
Representative γ-GCS sequences                                            [179]            [323]       [366]          [474]      [487] [491]
                      * *            *        *                             |            * |           |              |          | * |
Tb γGCS   48 FLWGDEIEH (33) WRPEYG-SFMVESL (66) PDACINDSHPRFK (136)NCLQLTMQL (38) VRWL (102)QTVRLK (10) RVEFRV 493 679
Hs γGCS   45 LKWGDEVEY (39) WRPEYG-SYMIEGT (70) PDEAIN-KHPRFS (60) CCLQVTFQA (38) CRWG (108)QTMRFK (10) RVEFRP 429 637
Dm γGCS   45 LKWGDEVEY (39) WRPEYG-AYMIEGT (71) PDEAIFPGHPRFK (52) CCLQLTFQA (38) CRWN (108)QTMRFK (10) RVEFRP 423 717
Ce γGCS   45 LKWGDEIEY (42) WRPEFG-SYMIEGT (60) PEQAVFLGHPRFK (62) CCLQVTFQA (38) SRWD (108)MNMRFK (11) RVEFRP 427 646
Sc γGCS   45 LFWGDELEY (39) FHPEYG-RYMLEAT (81) PDEVIN-RHVRFP (66) SCLQVTFQA (38) VRWN (130)QTLRFK (16) RVEFRP 474 678

Representative GS sequences                                                      271         321          344        355 359
                                                                                  |           |            |          |   |
St GS    124 VLFGPEPEF (76) HHHEVATAGQNEVA (43) -------------     SGMHCHMSL (45) KRLV (17) ASIRIP  (8) RIEVRF 361 468
Hs GS    129 PWFGMEQEY (55) TNAEVM-PAQWEFQ (44) -------------     AGCHTNFST (39) RRLT (19) ASIRIP  (9) YFEDRR 342 373
Dm GS    135 PWFGIEQEY (55) TNAEVM-PAQWEFQ (44) -------------     AGAHTNVST (39) RRLT (19) CSIRIP  (9) YFEDRR 348 369
Sc GS    126 IWFGLEQEY (55) INAEVM-PSQWEFQ (44) -------------     AGCHANVST (35) MRLT (19) SSIRIP  (9) YFEDRR 335 370
Mt GS    124 PWYGIEQEY (56) INGEVM-PGQWEFQ (44) -------------     AGAHTNYST (35) RRLT (19) ASIRVG  (9) YFEDRR 334 356
```

FIGURE 1: Sequence alignment of representative γ-GCS and GS sequences. The sequences were analyzed and aligned as described previously (*11*). The species name abbreviations are the following: Tb, *Trypanosoma brucei*; *Hs*, *human*; Dm, *Drosophila melanogaster*; Ce, *Caenorhabditis elegans*; Sc, *Saccharomyces cerevisiae*; St, *Salmonella typhimurium*; Mt, *Medicago truncatula*. Residues that are conserved in both families are displayed in boldface type. Metal binding residues are marked by a (*). The boxed numbers represent the *T. brucei* residue number for substrate binding determinants discussed in the text. The numbers above the GS sequences represent the numbering for the *Salmonella typhimurium* enzyme for which *t*he GS X-ray structures have been published (*13*, *20*). The heavy black line marks the loop sequence that is novel to the γ-GCS sequences and is implicated in L-Cys binding.

Table 1: Steady-State Kinetic Analysis of *T. brucei* γ-GCS Mutant Enzymes[a]

enzyme	k_{cat} (s^{-1})	K_m^{app}(L-Glu) (mM)	K_m^{app}(L-Aba) (mM)	K_m^{app}(ATP) (mM)
WT	3.9 ± 0.2	0.24 ± 0.02	10 ± 1	0.071 ± 0.010
R366A	0.32 ± 0.08	130 ± 6	34 ± 8	2.8 ± 0.9
R491A	0.055 ± 0.001	0.61 ± 0.04	nd	0.11 ± 0.01
T323A	0.79 ± 0.19	1.7 ± 0.3	7.5 ± 1.6	7.0 ± 0.5
R474A	0.24 ± 0.01	1.6 ± 0.0	56 ± 9	1.3 ± 0.1
R487A	1.2 ± 0.0	1.3 ± 0.0	15 ± 1	1.2 ± 0.1
R179A	0.61 ± 0.22	5.2 ± 0.4	380 ± 40	0.14 ± 0.02

[a] Rate data were collected by the spectrophotometric assay that follows ATP hydrolysis (Experimental Procedures). k_{cat} and K_m^{app} were obtained by fitting the rate data to the Michaelis−Menten equation. K_m^{app} values were collected with two substrates at fixed saturating concentrations while varying the third substrate. All fixed concentrations were 3−10-fold greater than K_m with several exceptions: fixed ATP was 5 mM in R366A and 10 mM in T323A; fixed L-Aba was 475 mM in R179A; and fixed L-Glu was 10 mM in R179A. k_{cat} value errors are standard deviations of the mean determined by averaging values from fits to each of the three substrates. K_m^{app} value errors are standard errors to the fit. k_{cat} and K_m^{app} data for wild-type *T. brucei* γ-GCS were taken from (*5*). nd: no significant dependence of the reaction rate on L-Aba concentration was detected.

only modestly (Table 1). However, while R491A γ-GCS catalyzed ATP hydrolysis is dependent on the concentration of L-Glu, it is not significantly dependent on the concentration of L-Aba.

To determine if R491A γ-GCS is capable of catalyzing dipeptide product formation, analysis of the reaction products by HPLC was undertaken (Figure 2A). This assay demonstrates that γ-glutamylaminobutyrate is formed during the course of the reaction catalyzed by R491A γ-GCS, but at a rate that is 20-fold slower than the rate of ATP hydrolysis under the same conditions. Previously (and in Table 4), we have demonstrated for the wild-type enzyme that the rate of ATP hydrolysis exactly corresponds to the rate of dipeptide product formation (*11*). Therefore, the tight coupling between ATP hydrolysis and dipeptide formation observed for the wild-type enzyme has been lost in the mutant enzyme, and only 5% of the hydrolyzed ATP is used for productive product formation. These data suggest that the role of R491 is to facilitate the nucleophilic attack of L-Aba on the γ-phosphorylated L-Glu intermediate during the second step of the reaction.

The K_m^{app} data in Table 1 provide information about the interaction of each substrate with enzyme saturated with the other two substrates. To understand the kinetic mechanism and interaction of substrate with free enzyme, a matrix of kinetic data was collected for the R366A *T. brucei* γ-GCS mutant by maintaining the concentration of one substrate at a constant, saturating level while varying the other two substrates in all combinations (Figure 3). These data were fitted to the rapid equilibrium rate equations that describe rapid equilibrium ter-reactant systems (*21*). The quality of the fit to the data was analyzed by statistical analysis of the standard error of the fitted parameters and the correlation coefficient (r^2). The data for R366A *T. brucei* γ-GCS, like wild-type γ-GCS, were best fit by the equation for a rapid equilibrium random ter-reactant system (eq 1, Figure 2). In this model, K_{ATP}, K_{Aba}, and K_{Glu} are the model-derived equilibrium dissociation constants for the respective substrates interacting with free enzyme, and α, β, and γ are the

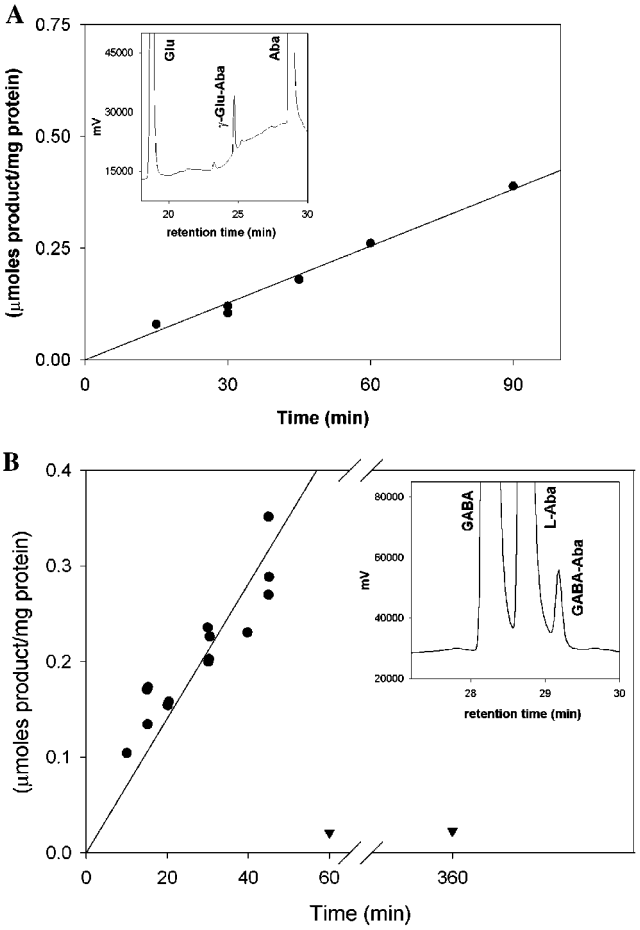

FIGURE 2: HPLC analysis of the reactions of mutant and wild-type γ-GCS. (A) The reaction of R491A with L-Glu. Plot of μmol of γ-Glu-Aba dipeptide product formed/mg of enzyme (circles) for reaction of enzyme with 20 mM L-Glu, 100 mM L-Aba, and 3 mM ATP. The inset shows the HPLC trace [mV recorded vs retention time (min)] of the 90 min time point for the reaction with 17 μM enzyme. (B) The reaction of R366A and wild-type γ-GCS with GABA as substrate. Plot of μmol of GABA-Aba dipeptide product formed/mg of enzyme versus time; R366A, circles; wild-type, triangles. Additional time points were collected at 120, 180, and 240 min for the wild-type enzyme; the results were the same as for the data points shown in the figure. The inset shows the HPLC trace for reaction of R366A (6 μM) with 5 mM ATP, 20 mM L-Aba, and 50 mM GABA at the 30 min time point. Retention times were used to identify the peaks, which are labeled on the chromatogram.

interaction factors that describe cooperativity among substrate-pairs.

The kinetic parameters obtained from this model reveal that mutation of R366 to Ala specifically affects L-Glu binding. The specific activity (V_{max}), K_{Aba}, and K_{ATP} were not significantly changed from the values obtained for the wild-type enzyme. However, K_{Glu} rises 160-fold to 420 ± 100 mM in R366A γ-GCS (Table 2), consistent with the large increase noted in K_m^{app} for L-Glu. Furthermore, mutation of R366 to Ala affects the cooperative binding interactions of ATP and L-Aba with L-Glu. The positive cooperativity observed between the binding sites of L-Glu and ATP in wild-type enzyme is lost in the R366A mutant enzyme (β increases 25-fold). Likewise, the negative cooperativity between the binding sites of L-Glu and L-Aba in wild-type enzyme disappears in the mutant (γ decreases 32-fold). However, α, the interaction factor between L-Aba and

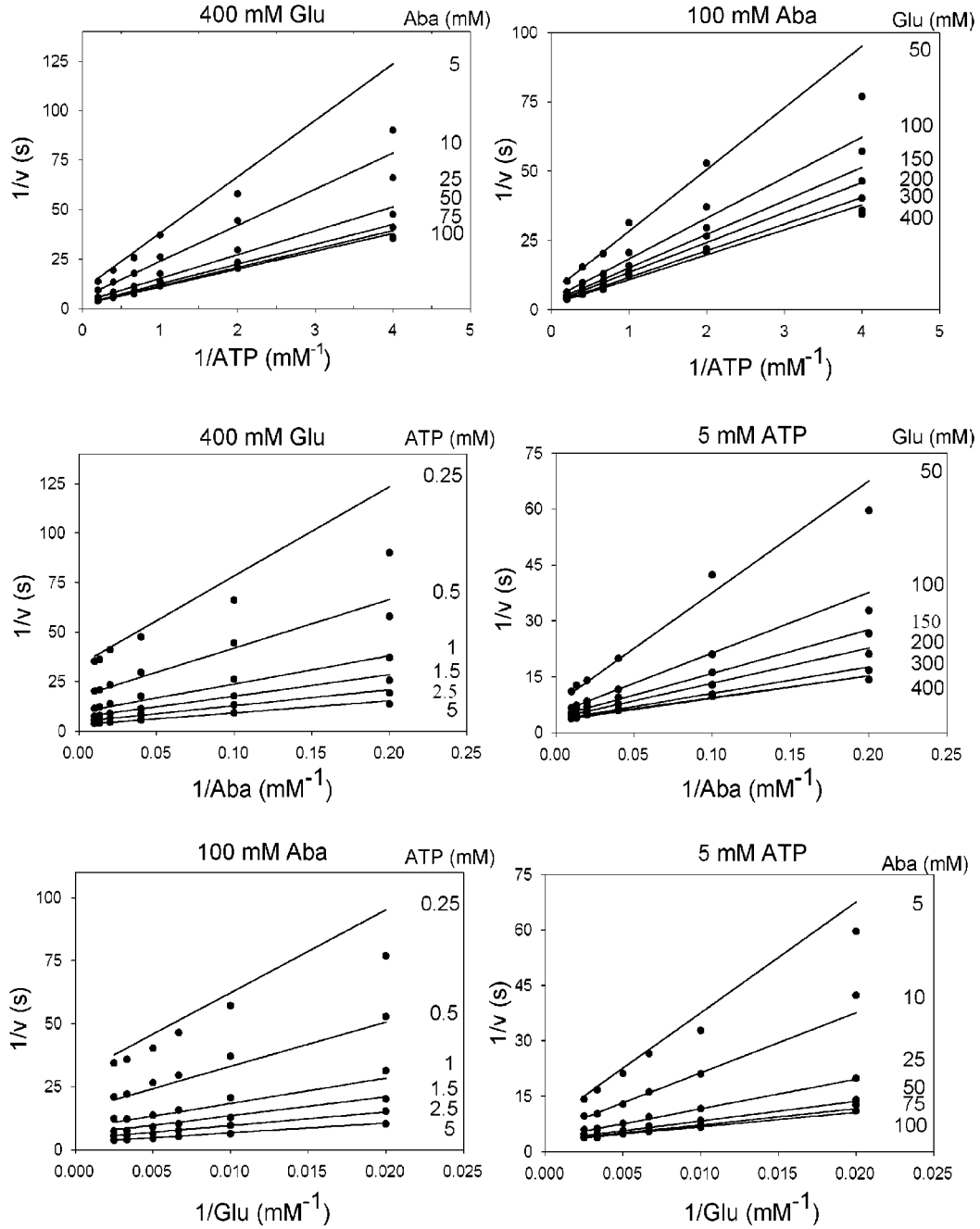

FIGURE 3: Lineweaver-Burk analysis of a representative data set for R366A *T. brucei* γ-GCS. Units are velocity in s^{-1} and substrate concentration in mM. The closed circles represent actual data points, and the lines represent the global fit of all data to eq 1, which models the random ter-reactant mechanism. Parameters of the fit are listed in Table 2. Reported errors are standard errors of the fit. The square of the correlation coefficient (r^2) for the global fit of all displayed data is 0.994.

ATP, does not change (Table 2). These data strongly suggest that R366 is a specific L-Glu binding determinant and is a crucial residue in mediating the cooperative interactions of L-Glu with the other substrates.

R366 Interacts with the α*-Carboxylate of L-Glu.* To further investigate potential binding deficits in the R366A mutant enzyme, two known γ-GCS inhibitors were tested. GSH, a competitive inhibitor that binds wild-type γ-GCS with a K_I of 1.1 mM (*5*), does not appreciably bind to the R366A mutant, and the K_I is increased by >220-fold. L-BSO is a time-dependent inhibitor of wild-type *T. brucei* γ-GCS, and the loss of enzyme activity upon incubation of L-BSO, ATP, and enzyme follows a single-exponential decay. The observed rate constants for the decay of activity (k_{obs}) were obtained for a range of BSO concentrations (1−5 μM) as described under Experimental Procedures. A linear dependence of k_{obs} on BSO concentration was observed, and the apparent second-order rate constant ($k_{inact}/K_I = 0.34\ \mu M^{-1}\ min^{-1}$) for inactivation by the inhibitor was calculated from the slope as described (*17*). In contrast to the results on the wild-type enzyme, BSO does not inhibit R366A γ-GCS even after incubation of the enzyme with 5 mM ATP and 40 mM L-BSO for 30 min at 37 °C. These data suggest either that BSO does not bind to the R366A mutant enzyme or that phosphorylation of the inhibitor is not catalyzed; thus, the high-affinity species cannot be formed. The inhibitor data indicate that R366 is an important binding determinant for two inhibitors, GSH and L-BSO, which both contain the

Table 2: Kinetic Constants for Wild-Type and Mutant *T. brucei* γ-GCS Based on Fits of the Data to the Random Ter-Reactant Model[a]

	wild-type γ-GCS	R366A γ-GCS	R487A γ-GCS
V_{max} (s^{-1})	2.6 ± 0.3	0.81 ± 0.05	1.0 ± 0.1
K_{Glu} (mM)	2.6 ± 2.0	420 ± 100	7.5 ± 5.6
K_{Aba} (mM)	5.4 ± 2.9	38 ± 7	28 ± 17
K_{ATP} (mM)	1.4 ± 1.2	2.2 ± 0.4	3.9 ± 2.8
α	0.93 ± 0.16	1.7 ± 0.3	1.1 ± 0.9
β	0.057 ± 0.024	1.4 ± 0.3	0.055 ± 0.034
γ	6.3 ± 1.2	0.2 ± 0.0	1.6 ± 1.3

[a] A representative fit to the R366A data is in Figure 2. K_{Glu}, K_{Aba}, and K_{ATP} are the model-derived equilibrium dissociation constants for the binding of the respective substrate to free γ-GCS. α is the interaction factor between L-Aba and ATP; β is the interaction factor between L-Glu and ATP; and γ is the interaction factor between L-Glu and L-Aba. All data for wild-type *T. brucei* γ-GCS are taken from (*6*). The errors for the R366A and R487A data are the standard error of the fits to eq 1. The errors for wild-type represent the standard error of the mean ($n = 3$).

Scheme 2

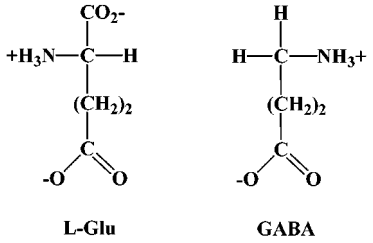

Table 3: Comparison of Wild-Type and R366A γ-GCS Steady-State Kinetics for ATP Hydrolysis with L-Glu versus GABA as Substrates[a]

	wild-type γ-GCS	R366A γ-GCS
k_{cat}(L-Glu) (s^{-1})	3.9 ± 0.2	0.32 ± 0.08
k_{cat}(GABA) (s^{-1})	0.14 ± 0.01	0.59 ± 0.02
K_m^{app}(L-Glu) (mM)	0.24 ± 0.02	130 ± 6
K_m^{app}(GABA) (mM)	150 ± 14	20 ± 3

[a] Rate data were collected by the spectrophotometric assay that follows ATP hydrolysis (Experimental Procedures). In all assays, the concentrations of ATP and L-Aba were 5 and 100 mM, respectively. L-Glu and GABA were varied over their dynamic concentration ranges. Errors are the standard error of the fit to the Michaelis−Menten equation. The wild-type data with L-Glu as substrate are from (*5*).

L-Glu moitey and in both cases contain a free α-carboxylate, but not a free γ-carboxylate.

To further examine the question of whether R366 interacts with the α- or γ-carboxylate of L-Glu, GABA, a structural analogue of L-Glu with a hydrogen in place of the α-carboxylate (Scheme 2), was used as a replacement for L-Glu in the reactions catalyzed by wild-type and R366A γ-GCS. R366A γ-GCS hydrolyzes ATP in the presence of GABA with a 2-fold higher k_{cat} and with a 7-fold lower K_m^{app} than was observed with L-Glu (Table 3). Wild-type γ-GCS, in contrast, did not use GABA as efficiently as L-Glu; the ATP hydrolysis rate is 28-fold lower and the K_m^{app} for GABA is 600-fold higher than observed for L-Glu. However, the ability of the *T. brucei* wild-type enzyme to stimulate ATP hydrolysis in the presence of GABA distinguishes it from the rat enzyme, which has been reported to be unable to catalyze this reaction (*10*). Notably, the reactions observed in the presence of GABA were independent of L-Aba concentration for both wild-type and R366A γ-GCS, suggesting that GABA was stimulating ATP hydrolysis without forming dipeptide product.

Table 4: Comparison of Wild-Type and R366A γ-GCS Steady-State Kinetics with L-Glu or GABA as Substrates: ATP Hydrolysis Rates versus Dipeptide Product Formation Rates

	wild-type γ-GCS	R366A γ-GCS
(A) ATP Hydrolysis Rates		
L-Glu (s^{-1})	0.52 ± 0.03	0.035 ± 0.003
GABA (s^{-1})	0.021 ± 0.001	0.12 ± 0.01
(B) Dipeptide Product Formation Rates		
L-Glu (s^{-1})	0.50 ± 0.10	0.035 ± 0.008
GABA (s^{-1})	nd	0.0088 ± 0.0026

[a] (A) Rate data were collected by the spectrophotometric assay that follows ATP hydrolysis (Experimental Procedures). (B) Dipeptide product formation (γ-glutamylaminobutyrate or GABA-Aba) was followed by HPLC (see Experimental Procedures; Figure 2B). All reactions took place in a different buffer (40 mM MOPS, pH 8.0, 20 mM NaCl, 5 mM $MgCl_2$) from data reported in Tables 1−3. In addition, ATP concentrations were 5 mM, and L-Aba levels were at 20 mM, a nonsaturating concentration. For wild-type and R366A γ-GCS, L-Glu concentrations were 10 and 200 mM, respectively. For wild-type and R366A γ-GCS, GABA concentrations were 100 and 50 mM, respectively. All errors are standard deviations of the mean [(A) $n = 3$; (B) $n = 6-12$]. nd, not detected; GABA-Aba formation was not detected upon reaction of 60 μM wild-type γ-GCS with substrate over a time course of 2−6 h at 37 °C.

To investigate whether ATP hydrolysis in the presence of GABA was coupled with dipeptide product formation, HPLC was used to follow dipeptide product formation (Figure 2B). For both wild-type and R366A γ-GCS, the rate of dipeptide formation with L-Glu as the substrate was the same as the rate of ATP hydrolysis. However, when GABA is substituted for L-Glu in the reaction, the wild-type enzyme does not produce any detectable dipeptide (GABA-Aba) product. In contrast, R366A γ-GCS produced the GABA-Aba product at a detectable rate, although it was 14-fold slower than the ATP hydrolysis rate measured under the same conditions (Table 4). Since removal of both charges could be expected to compensate for the detrimental effects that are observed when only one of the charge pair partners is removed, these data suggest that R366 interacts with the α-carboxylate of L-Glu.

ATP Binding Determinants in T. brucei γ-GCS: Kinetic Analysis of T323A, R474A, and R487A. The X-ray structures of GS identify a number of residues that contact the phosphate groups of ATP (*13*). Of these residues, only R474 (in *T. brucei* γ-GCS), which interacts with the β-phosphate in GS, is invariant in both the GS and γ-GCS families (Figure 1). In the GS structure, the α-phosphate group makes contacts with two residues that conserve hydrogen-bonding potential, but that are not invariant within either family (T323 and R487 in *T. brucei* γ-GCS; Figure 1). To test if these residues are also involved in ATP binding in the γ-GCS family, all three residues were mutated to Ala, and the purified mutant enzymes were analyzed. Mutation of any one of these residues to Ala significantly increases the apparent K_m for ATP, modestly increases the K_m^{app} for L-Glu, and does not alter the K_m^{app} for L-Aba (Table 1). Of these mutations, only the R474A mutation causes a significant decrease in k_{cat}. The kinetic mechanisms of the R474A and the R487A mutant enzymes were analyzed by collecting a full matrix of kinetic data as described for R366A (Figure 3). For R487A γ-GCS, the data were well fit to the rapid equilibrium random ter-

reactant model. The kinetic parameters for substrate binding were within 3−5-fold of those obtained for the wild-type enzyme (Table 2), suggesting only a modest role for this residue in substrate binding. In contrast, the data for R474A γ-GCS were not well fit to a rapid equilibrium random ter-reactant model, suggesting a change in mechanism for the mutant enzyme. The data were better fit by an ordered B mechanism (*21*). However, an equally good fit was obtained when the B substrate was defined as either L-Aba or L-Glu. Therefore, this method does not provide conclusive mechanistic information about the role of R474 and does not provide for a direct comparison of substrate kinetic parameters with the wild-type enzyme. However, the finding that this mutation causes a 20-fold decrease in k_{cat} while affecting the reaction mechanism supports a role for this residue in the reaction.

Based on the structure of GS bound to ADP, T323 is predicted to bind the α-phosphate of ATP and to be near, although not a direct ligand of, the n2 metal in the active site (*13*). The metal dependency of the reaction rate of T323A γ-GCS was monitored in order to understand any changes in metal dependency of the mutant enzyme. The concentrations of free metal were calculated from total metal and ATP concentrations by using the computer program "Bound and Determined" (*16*). A hyperbolic dependence of reaction rate on free Mg^{2+} and Mn^{2+} was observed. The data were fitted to the Michaelis−Menten equation. The apparent K_d (7.3 ± 2.1 mM) for free Mg^{2+} was 14-fold higher for T323A than for wild-type γ-GCS, and the K_d^{app} (0.03 ± 0.01 mM) for free Mn^{2+} increased 5-fold. Furthermore, the k_{cat} in the presence of Mn^{2+} is 6.0 ± 0.5 s^{-1}, roughly 3-fold higher than for wild-type *T. brucei* γ-GCS and 8-fold higher than T323A γ-GCS activated by Mg^{2+}.

R179 Is an L-Aba Binding Determinant in T. brucei γ-GCS: Steady-State Analysis and GSH Binding. GS is thought to bind the third substrate ammonia using residues from adjacent subunits (*13*). Previous gel filtration analysis indicated that *T. brucei* γ-GCS is a monomer (*5*); thus, active site interactions across subunit boundaries could not contribute to enzyme function. To further test this hypothesis, wild-type *T. brucei* γ-GCS was analyzed by analytical ultracentrifugation in the presence and absence of Mg^{2+} and Mn^{2+} (Experimental Procedures). The data obtained for three protein concentrations and three rotor speeds were globally fitted to various models, including a single ideal species and various oligomeric models. The data were best fit to a monomer−dimer equilibrium with a dimer dissociation constant in the range of K_d = 15−30 μM for all conditions tested, with or without divalent metal (Figure 4). These data indicate that the functional form of γ-GCS is a monomer, since the γ-GCS dimer forms only at concentrations significantly above the concentrations required for full enzyme activity (the concentration of γ-GCS used in a standard assay is 0.1−0.4 μM).

Based on the finding that γ-GCS is a functional monomer, the L-Cys binding site must be contained within a single chain. Thus, differences between the GS and γ-GCS families, particularly the conserved insertions in the γ-GCS family compared to the GS family, may indicate the location of the L-Cys binding site. The γ-GCS family contains an insert (residues 162−189) that is not present in GS containing an invariant Arg (R179) residue (Figure 1). This motif maps to a predicted loop immediately before strand b4, which contains one of the n2 metal ligands (Q321), and would be positioned based on the GS structure adjacent to the active site cleft of the other two substrates (*11*). We hypothesize that the conserved Arg residue may function as an L-Cys binding determinant by interacting with its carboxyl group. Mutation of R179 to Ala decreases the k_{cat} 6-fold and increases the K_m^{app}'s for L-Aba and L-Glu by 22- and 38-fold, respectively (Table 1). Furthermore, the K_I for GSH increases 33-fold to 36 ± 3 mM, revealing a ligand binding deficit in the mutant enzyme. R179A γ-GCS displays substrate inhibition with both ATP and L-Aba when only one other substrate is saturating. This effect is not seen when obtaining K_m^{app} data at saturating concentrations of the remaining two ligands, suggesting that mutating R179 to Ala alters the active site and effects the substrate dependencies. For this reason, it was not possible to analyze the kinetic mechanism of this mutant as described for R366. The data suggest a role for this residue in mediating interactions with L-Glu or L-Aba or in promoting the cooperative interaction between these substrates.

Ala Scanning Mutagenesis and Kinetic Analysis of Conserved, Basic Residues in T. brucei γ-GCS. An amino acid sequence alignment of eukaryotic γ-GCS identifies other conserved, basic residues that may have a role in substrate binding and/or catalysis (*11*). Eight other conserved Arg residues and one other conserved Lys residue were mutated to Ala by site-directed mutagenesis. R124A and R612A were not expressed as soluble proteins. R190A, R191A, R377A, R389A, R441A, R625A, and K194A were expressed and purified, but all had kinetic parameters similar to wild-type γ-GCS. These data suggest that these residues play no significant role in substrate binding or catalysis, consistent with the fact that these residues are conserved in eukaryotic, but not in prokaryotic, γ-GCS's (*11*).

DISCUSSION

This paper presents data that for the first time elucidate determinants of substrate binding in the active site of γ-GCS and establish the roles of several key residues in the reaction chemistry. Considered along with recent observations that γ-GCS shares a common fold with GS, and with the recent analysis of the two metal binding sites (*11*), a more complete model of the active site of γ-GCS can be proposed (Figure 5). In this model, the α-carboxylate of L-Glu interacts with R366; R491 interacts with the γ-carboxylate of L-Glu and is important in catalyzing peptide bond formation, and the phosphate groups of ATP interact with T323 and R474. These residues all play important roles in the catalytic function and substrate binding of γ-GCS.

These studies demonstrate an important role of R366 in forming interactions with the α-carboxylate of L-Glu in γ-GCS. Mutation of R366 to Ala in γ-GCS significantly increased the kinetically determined binding constant for L-Glu, while having little effect on the binding constants for the other substrates. Furthermore, mutation of R366 to Ala uncoupled the cooperative binding interactions that were observed for the wild-type enzyme between L-Glu and the other substrates. ATP and L-Glu have a favorable interaction energy (β) in wild-type γ-GCS of 1.7 kcal/mol. In contrast,

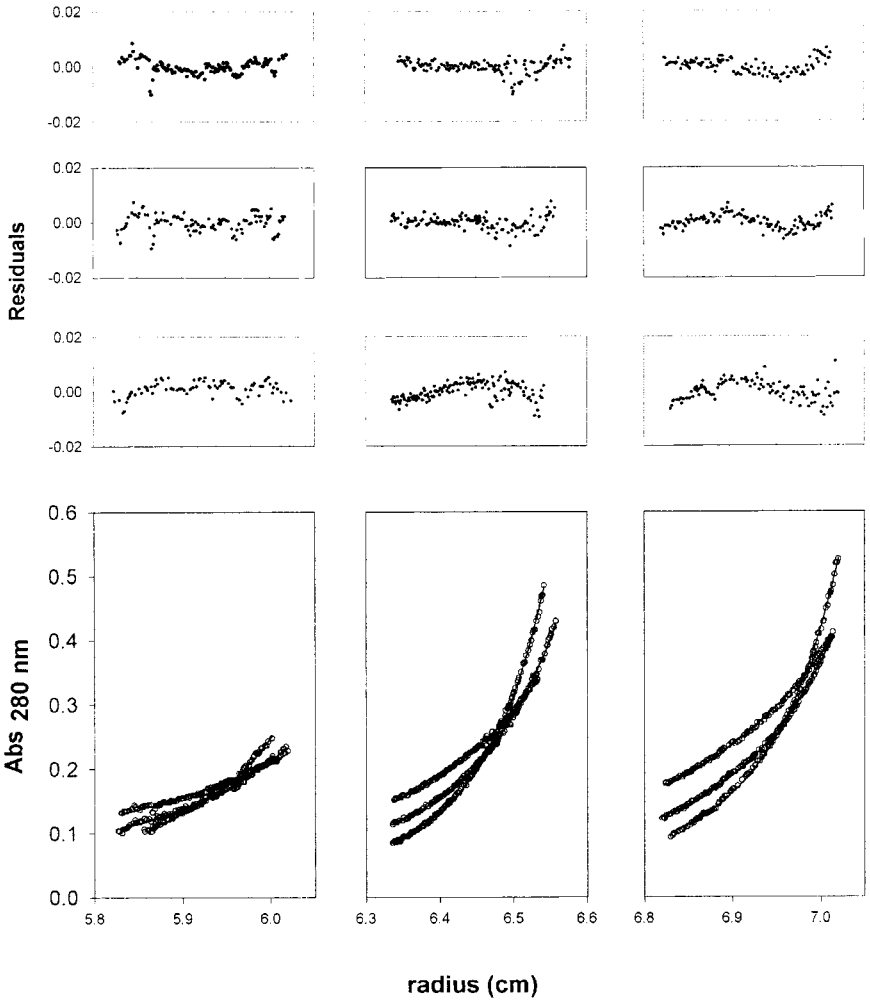

FIGURE 4: Analytical ultracentrifugation of wild-type γ-GCS. Equilibrium sedimentation data were collected for wild-type γ-GCS in the presence of Mg^{2+} as described under Experimental Procedures. The data in the figure include nine data sets (open circles) used in the global analysis fitted to the model for a monomer−dimer equilibrium (solid line) with a $K_d = 34$ μM and 95% confidence interval of 29−41 μM. The panels (from left to right) represent data collected for three γ-GCS concentrations (3.4, 4.5, and 6.8 μM) and for three rotor speeds (from left to right: 8000, 10 000, and 12 000 rpm). The residuals to the fit are shown in the upper panel.

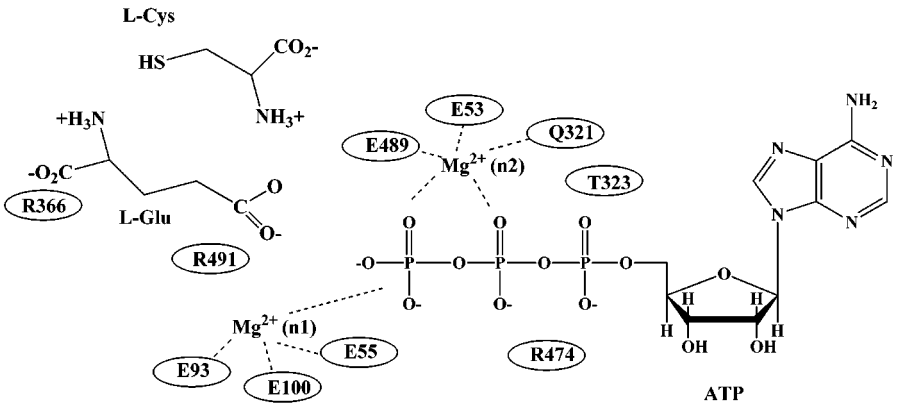

FIGURE 5: Model of the γ-GCS active site. The model is based upon data from this paper, previous data on metal binding residues, and a structural schematic of the active site of GS (*11*).

for R366A to Ala γ-GCS, this interaction has been weakened by 1.9 kcal/mol, while the interaction energy between L-Glu and L-Aba changes from an unfavorable interaction energy of 1.1 kcal/mol in wild-type γ-GCS to a favorable interaction energy of 1 kcal/mol in R366A γ-GCS. These results are based on a random ter-reactant model for the reaction kinetics, and they suggest that the mutant enzyme is impaired in its ability to bind L-Glu and to promote interactions with the other substrates. The inability of GSH and L-BSO to inhibit the mutant enzyme further confirms that R366A γ-GCS possesses a major ligand binding deficit.

The inhibitor data suggest that R366 most likely binds L-Glu through its α-carboxylate group, because both GSH and BSO retain the α-carboxylate but lack the γ-carboxylate of L-Glu. In further support of this hypothesis, R366A γ-GCS is able to stimulate ATP hydrolysis more efficiently

with GABA than L-Glu, while the wild-type enzyme has the opposite specificity. Furthermore, dipeptide product (GABA-Aba) is not formed with wild-type γ-GCS, but it is formed by the R366A mutant, albeit at a rate less than 10% the rate of ATP hydrolysis. Thus, substitution of the α-carboxylate of L-Glu with hydrogen in GABA can complement the R366A enzyme mutation, suggesting that binding an unpaired charged group in the active site of the mutant enzyme is unfavorable. Removal of this group in the GABA analogue provides for a more favorable interaction. R366 aligns with R321 of GS in a multiple sequence alignment of the γ-GCS and GS families (*11*). Although no mutational analyses have been reported for R321 in GS, the X-ray crystal structure of *Salmonella typhimurium* GS shows that this residue interacts with the α-carboxylate of L-Glu (*13*). This role for the analogous residue in GS, combined with these kinetic data, confirms a role for R366 in binding the α-carboxylate of L-Glu in γ-GCS.

R491 has been identified as a second important residue in the L-Glu binding site. Mutation of R491 to Ala significantly affected the catalytic mechanism of γ-GCS. Dipeptide product is formed in only 5% of the ATP hydrolysis events catalyzed by the mutant enzyme. Furthermore, the rate of dipeptide product formation has been reduced by 1400-fold, revealing a large catalytic deficit in this step of the reaction. In contrast, the ATP hydrolysis rate has only been reduced by 70-fold. Thus, ATP hydrolysis and dipeptide product formation have been largely uncoupled by the mutation. The analogous residue in GS is positioned near the γ-carboxylate of L-Glu (*13*), suggesting that the role of R491 is to interact with the γ-carboxylate and stabilize the oxyanion formed in the transition state during dipeptide product formation. The effects of mutating R491 are similar to what was observed upon mutation of E93 in *T. brucei* γ-GCS (*11*). E93 ligates the n1 metal, which is also implicated in interactions with the γ-carboxylate of L-Glu (Figure 5).

The ATP binding site of γ-GCS is predicted to contain residues T323, R474, and R487, based on the X-ray structure of GS bound to ATP analogues (*13*, *20*). Mutation of all three residues resulted in enzymes with impaired catalytic function and specifically diminished apparent ATP binding affinity. However, more detailed kinetic analysis of R487 did not support a strong role for ATP binding by this residue. Beyond the changes in the K_m^{app} for ATP, T323A γ-GCS also exhibited mild changes in divalent metal activation as the apparent K_d for free Mg^{2+} increased in the mutant enzyme. These data are consistent with the proposed role of the analogous residue (H271) in GS. The X-ray crystal structure of GS reveals that H271 binds the α-phosphate of ATP and is near, although not a direct ligand to, the n2 metal (*13*, *20*). R474 interacts with the β-phosphate of ATP in the GS structure (*13*, *20*). In addition to affecting the apparent binding affinity of ATP, mutation of R474 in γ-GCS altered the reaction mechanism, such that the data were no longer well fit by a random ter-reactant model. These data support a role for this residue in interactions with ATP.

While the GS structure provides significant insight into the L-Glu and ATP binding sites of γ-GCS, the nature of the L-Cys binding site is much less clear. Differences between the two enzyme families with regard to binding of the third ligand are, however, evident. While GS is an oligomer that utilizes residues from an adjacent subunit to form the binding site for ammonia (*15*), the analytical ultracentrifugation data clearly demonstrate that γ-GCS is a monomer and thus must utilize residues from a single chain to form its entire active site. In the alignment of eukaryotic and prokaryotic γ-GCS sequences, R179 is strictly conserved and maps to an insert not present in GS (*11*), features that make R179 a candidate residue to bind the α-carboxyl group of L-Cys. In support of this hypothesis, the R179A mutation caused significant deficits in ligand binding: GSH is bound 33-fold more weakly to the mutant enzyme than to wild-type γ-GCS. In addition, the apparent K_m's for L-Glu and L-Aba were both increased, and substrate inhibition patterns that are not present in the wild-type enzyme were observed. The data suggest that R179 may form part of the binding site for the third ligand and suggest a role for this region in formation of the substrate binding sites in γ-GCS. Conformation of this hypothesis awaits structural analysis of the γ-GCS family.

ACKNOWLEDGMENT

We thank Dr. Nick Grishin, Jimin Pei, and Dr. David Myers for helpful discussions.

REFERENCES

1. Griffith, O. W., and Mulcahy, R. T. (1999) The enzymes of glutathione synthesis:γ-glutamylcysteine synthetase. in *Advances in Enzymology and Related Areas of Molecular Biology* (Purich, D., Ed.) pp 209−267, John Wiley & Sons, New York.
2. Fairlamb, A. H., and Le Quesne, S. A. (1997) Polyamine metabolism in Trypanosomes. in *Trypanosomiasis and Leishmaniasis* (Hide, G., et al., Eds.) pp 149−161, CAB International, Wallingford, Oxon, U.K.
3. Mehlotra, R. K. (1996) *Clin. Rev. Microbiol. 22*, 295−314.
4. Arrick, B. A., Griffith, O. W., and Cerami, A. (1981) *J. Exp. Med. 153*, 720−725.
5. Lueder, D. V., and Phillips, M. A. (1996) *J. Biol. Chem. 271*, 17485−17490.
6. Brekken, D. L., and Phillips, M. A. (1998) *J. Biol. Chem. 273*, 26317−26322.
7. Orlowski, M., and Meister, A. (1971) *J. Biol. Chem. 246*, 7095−7105.
8. Griffith, O. W., Anderson, M. E., and Meister, A. (1979) *J. Biol. Chem. 254*, 1205−1210.
9. Griffith, O. W. (1982) *J. Biol. Chem. 257*, 13704−13712.
10. Sekura, R., and Meister, A. (1977) *J. Biol. Chem. 252*, 2599−2605.
11. Abbott, J. J., Pei, J., Ford, J. L., Qi, Y., Grishin, V. N., Pitcher, L. A., Phillips, M. A., and Grishin, N. V. (2001) *J. Biol. Chem. 276*, 42099−42107.
12. Eisenberg, D., Gill, H. S., Pfluegl, G. M., and Rotstein, S. H. (2000) *Biochim. Biophys. Acta 1477*, 122−145.
13. Liaw, S. H., and Eisenberg, D. (1994) *Biochemistry 33*, 675−681.
14. Dhalla, A. M., Li, B., Alibhai, M. F., Yost, K. J., Hemmingsen, J. M., Atkins, W. M., Schineller, J., and Villafranca, J. J. (1994) *Protein Sci. 3*, 476−481.
15. Alibhai, M., and Villafranca, J. J. (1994) *Biochemistry 33*, 682−686.
16. Brooks, S. P. J., and Storey, K. B. (1992) *Anal. Biochem. 201*, 119−126.
17. Kitz, R., and Wilson, I. B. (1962) *J. Biol. Chem. 237*, 3245−3249.

18. Liu, H. J., Chang, B. Y., Yan, H. W., Yu, F. H., and Liu, X. X. (1995) *J. AOAC Int. 78*, 736−744.
19. Laue, T. M., Shah, B., Ridgeway, T. M., and Pelletier, S. L. (1992) Computer-aided interpretation of analytical sedimentation data for proteins. in *Analytical Ultracentrifugation in Biochemistry and Polymer Science* (Harding, S., Rowe, A., and Horton, J., Eds.) pp 90−125, Royal Society of Chemistry, Cambridge, U.K.
20. Liaw, S. H., Jun, G., and Eisenberg, D. (1994) *Biochemistry 33*, 11184−11188.
21. Segel, I. H. (1975) *Enzyme kinetics, behavior and analysis of rapid equilibrium and steady-state enzyme systems* (Segel, I., Ed.) John Wiley & Sons, Inc., New York.

BI0159128